Electronic Supplementary Material (ESI) for Journal of Materials Chemistry A.
This journal is © The Royal Society of Chemistry 2020

Supplementary information

Enabling Electrochemical N_2 Reduction to NH_3 in the Low Overpotential Region Using Non-Noble Metal Bi Electrodes via Surface Composition Modification

Youn Jeong Jang[1,2] and Kyoung-Shin Choi[1,*]

[1]Department of Chemistry, University of Wisconsin-Madison, Madison, WI 53706, United States
[2]Department of Chemical Engineering, University of Hanyang, Seongdong-gu, Seoul, 04763, Republic of Korea

* Correspondence and requests for materials should be addressed to K.-S.C.

(email: kschoi@chem.wisc.edu).

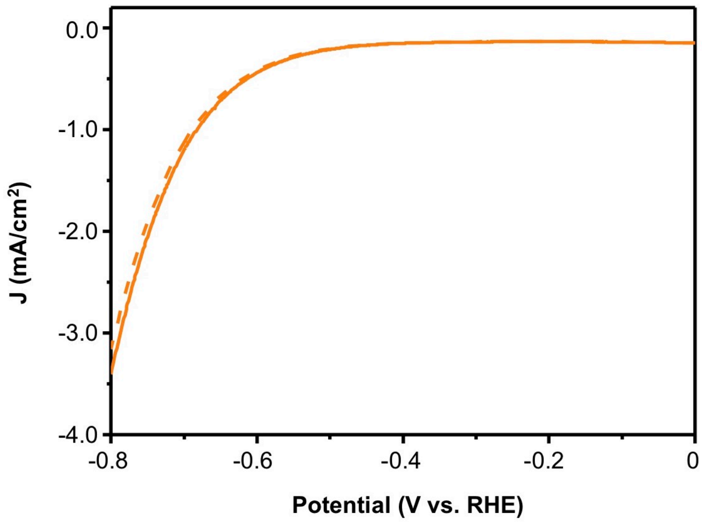

Figure S1. LSVs of a p-Bi electrode obtained in 0.5 M phosphate buffer (pH 7.5) saturated with N_2 (solid) or Ar (dashed) after applying -0.3 V vs. RHE for 1 min to remove the surface Bi_2O_3 layer (scan rate: 10 mV/s).

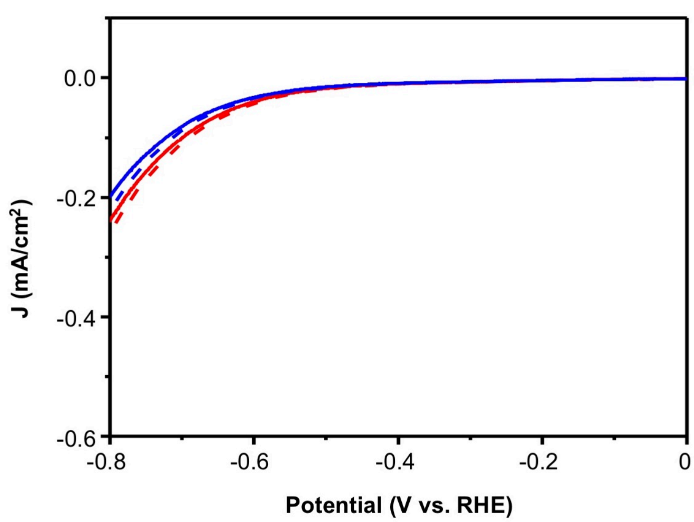

Figure S2. LSVs of the Ti foil used as the substrate to deposit p-Bi electrode obtained in 0.5 M phosphate buffer (pH 7.5) saturated with N_2 (solid) or Ar (dashed) with (blue) and without (red) 25 mM V_2O_5 (scan rate: 10 mV/s).

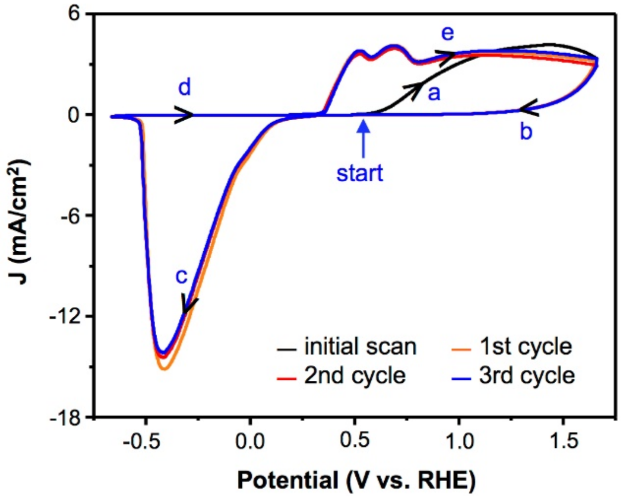

Figures S3. The CV treatment performed on a p-Bi electrode in 0.5 M phosphate buffer (pH 7.5) (scan rate: 25 mV/s). The potential was initially swept from the OCP to 1.62 V vs. RHE (denoted as a) and then cycled between 1.62 V vs. RHE and -0.65 V vs. RHE (b → c → d → e) three times and ended at 1.62 V vs. RHE.

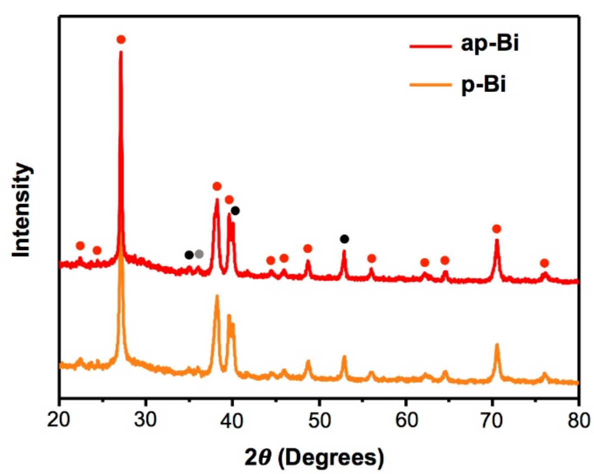

Figure S4. XRD patterns of p-Bi and ap-Bi electrodes. The peaks generated by Bi (JCPDS No: 85-1329) are indicated by red dots. The Ti (JCPDS No: 44-1294) and TiO_2 (JCPDS No. 34-0180) peaks from a Ti substrate are indicated by black and gray dots, respectively.

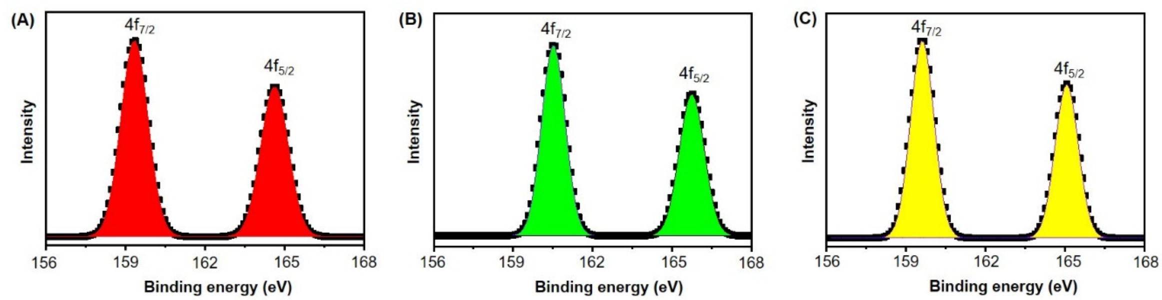

Figure S5. Bi 4f XPS spectra of (A) Bi_2O_3 (Aldrich, 99.999 %), (B) $BiPO_4$ (Aldrich, 99.99 %) and (C) $BiVO_4$ (prepared using the method reported in Ref. 36 in the main text) used as references to index the Bi spectra shown in Figures 1C-D, 4C and 5C.

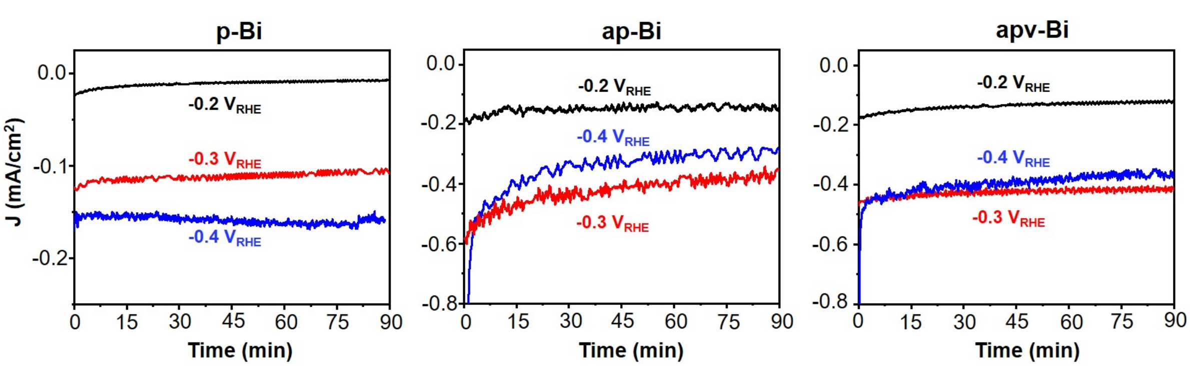

Figure S6. J-t profiles of p-Bi, ap-Bi, and apv-Bi electrodes during ENRR at various potentials in N_2 saturated phosphate buffer (pH 7.5).

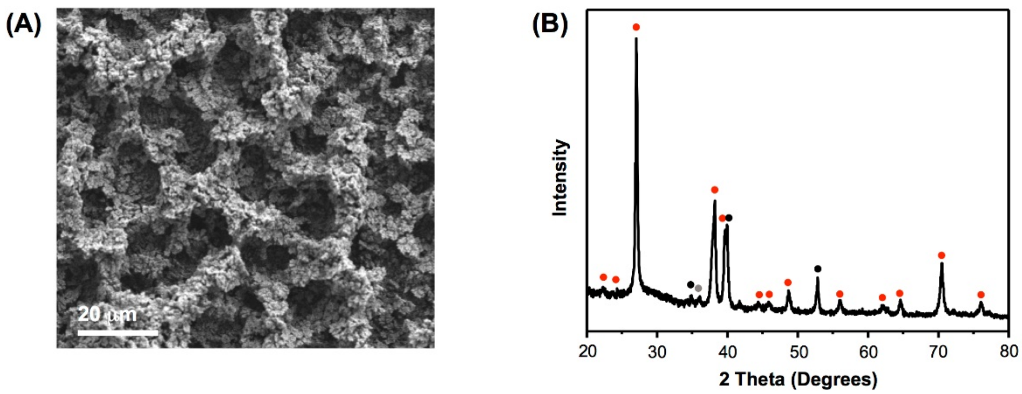

Figure S7. (A) SEM image and (B) XRD pattern of an apv-Bi electrode. The peaks generated by Bi (JCPDS No: 85-1329) are indicated by red dots. The Ti (JCPDS No: 44-1294) and TiO_2 (JCPDS No. 34-0180) peaks from a Ti substrate are indicated by black and gray dots, respectively.

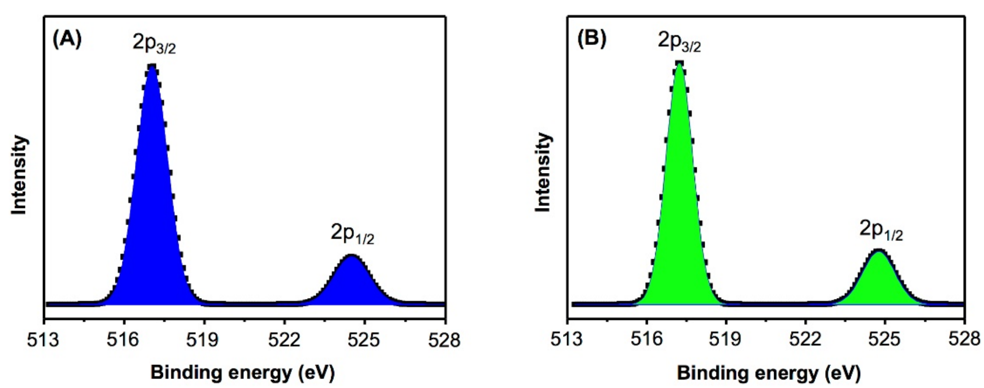

Figure S8. V 2p XPS spectra of (A) $BiVO_4$ and (B) $VOPO_4$ used as references to index V peaks shown in Figures 4E and 5D.

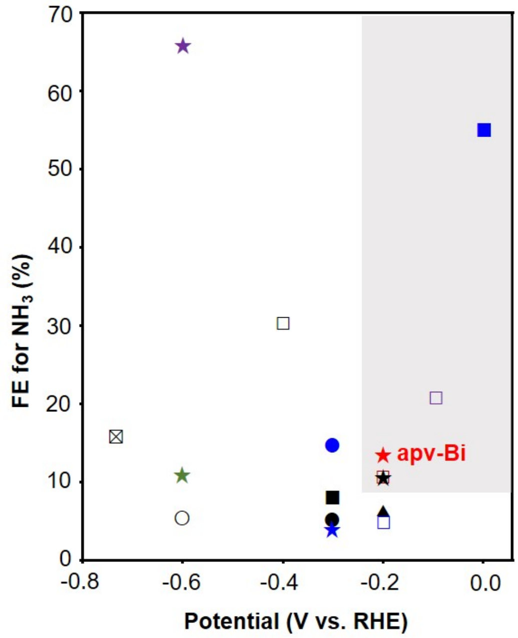

Category	Symbol	Catalyst	F.E. % (Poten.)	Electrolyte (pH)	Reference
Noble Metal	□	Au nanocage	30.2 %(-0.4 V_{RHE})	0.5 M $NaClO_4$	Nanoenergy, 2018, 49, 316
	□	a-Au NP/RGO	10.1 % (-0.2 V_{RHE})	Diluted HCl (pH 1)	Adv. Mater. 2017, 29, 1700001
	□	THH-Au NR	4.0 % (-0.2 V_{RHE})	0.1 M KOH (pH 13)	Adv. Mater. 2017, 29, 1604799
	□	Au NP/NCM	22.0 % (-0.1 V_{RHE})	0.1 M HCl (pH 1)	Angew. Chem. In. Ed. 2018, 57, 12360
	○	Ag nanosheet	4.8 % (-0.6 V_{RHE})	0.1 M HCl (pH 1)	Chem. Commun. 2018, 54, 11427
Non-Noble Metal	●	Mo_2N	4.5 % (-0.3 V_{RHE})	0.1 M HCl (pH 1)	Chem. Commun. 2018, 54, 8474
	●	Mo atom	14.6 % (-0.3 V_{RHE})	0.1 M KOH (pH 13)	Angew. Chem. Int. Ed. 2019, 58, 2321
	■	Fe/Fe_3O_4	8.29 % (-0.3 V_{RHE})	0.5 M KH_2PO_4 (pH 7.5)	ACS Catal. 2018, 8, 9312
	■	Fe-N-C	56.55 % (0.0 V_{RHE})	0.1 M KOH (pH 13)	Nat. Commun. 2019, 10:341
	▲	VN	6.5 % (-0.2 V_{RHE})	N_2-H_2 (1 atm, 0.1 L/min)	J. Am. Chem. Soc. 2018, 140, 13387
	★	a-$Bi_4V_2O_{11}$	10.16 % (-0.2 V_{RHE})	Diluted HCl (pH 1)	Angew. Chem. Int. Ed. 2018, 57, 6073
	★	defective Bi	11.68 % (-0.6 V_{RHE})	0.2 M Na_2SO_4	Angew. Chem. Int. Ed. 2019, 58, 1
	★	Bi NC	66 % (-0.6 V_{RHE})	0.5 M K_2SO_4 (pH 3.5)	Nat. Catal. 2019, 2, 448
	★	p-Bi	3.7 % (-0.3 V_{RHE})	0.5 M KH_2PO_4 (pH 7.5)	This work
	★	apv-Bi	13.2 % (-0.2 V_{RHE})	0.5 M KH_2PO_4 (pH 7.5)	This work
Metal free	⊠	B_4C	15.95 % (-0.75 V_{RHE})	Diluted HCl (pH 1)	Nat. Commun. 2018, 9:3485

Figure S9. Literature survey of the highest FEs for NH_3 production reported to date. A table summarizing the performances is also shown. Any study that reports NH_3 production at a potential where NH_3 production is thermodynamically not possible is not included. The shaded region shows the catalysts that achieved a FE for NH_3 production greater than 10% at a potential ≤ -0.2 V vs. RHE.

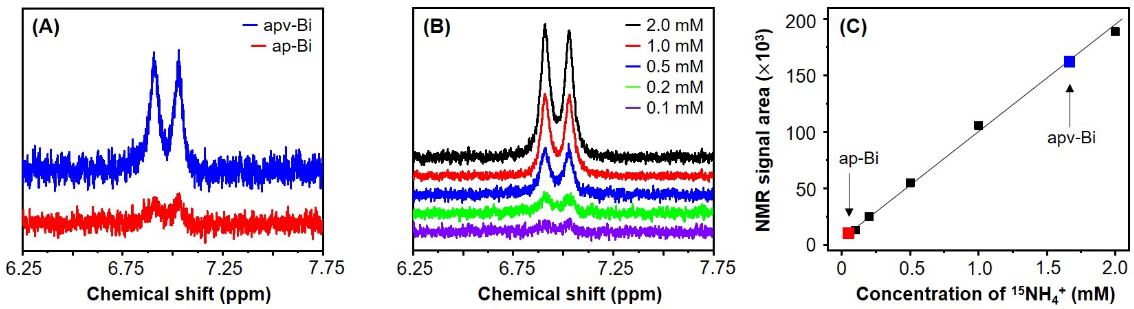

Figure S10. (A) ^{1}H-NMR spectra of $^{15}NH_4^+$ produced by ENRR using the ap-Bi and apv-Bi electrodes at -0.2 V vs. RHE; (B) ^{1}H-NMR spectra of $^{15}NH_4^+$ in standard solutions and (C) the resulting calibration curve.

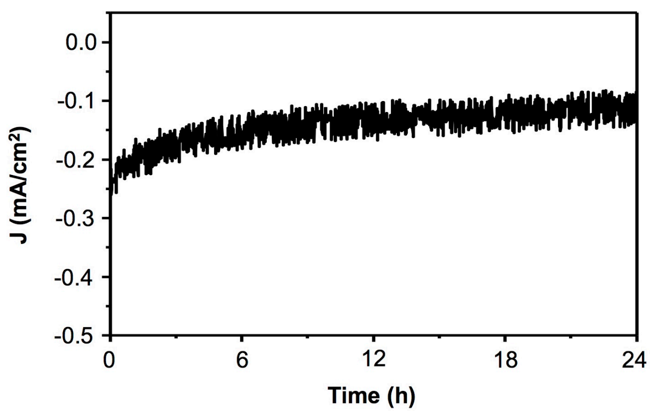

Figure S11. The J-t plot of the apv-Bi at -0.2 V vs RHE for 24 hours in N_2-saturated phosphate buffer (pH 7.5) containing 25 mM V_2O_5. The FE for NH_3 production obtained from this experiment was 11.7%.

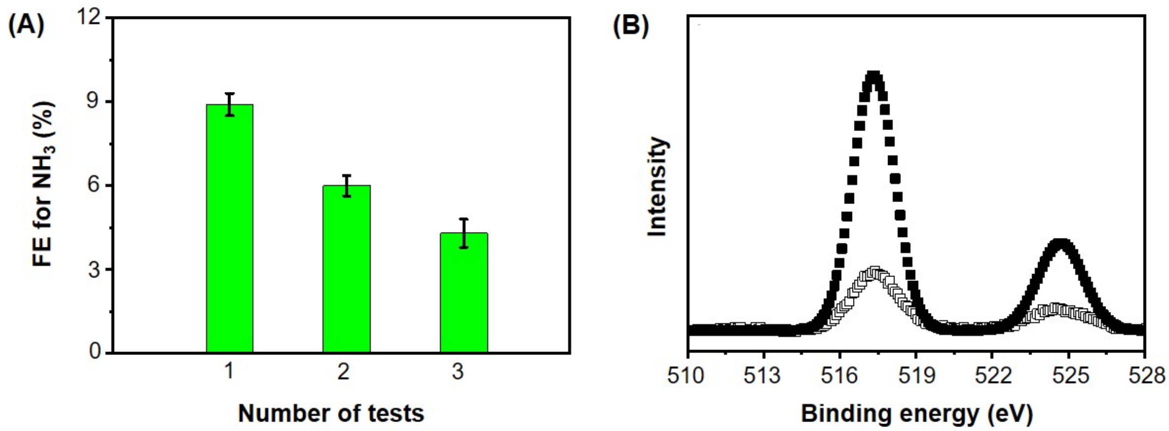

Figure S12. (A) Changes in FE for NH_3 production of an apv-Bi electrode for repeated ENRR at -0.2 V vs. RHE in 0.5 M phosphate buffer (pH 7.5) without 25 mM V_2O_5. (B) V 2p XPS spectrum of an apv-Bi electrode before (filled squares) and after (empty squares) repeating ENRR 3 times at -0.2 V vs. RHE in 0.5 M phosphate buffer (pH 7.5) without 25 mM V_2O_5.

Table S1. Yields and production rates of NH_3 obtained by p-Bi, ap-Bi, and apv-Bi electrodes in N_2-saturated phosphate buffer (pH 7.5).

Potential V vs RHE	**Yield (μg/cm²)**			**Production rate (μg/cm²·h)**		
	p-Bi	**ap-Bi**	**apv-Bi**	**p-Bi**	**ap-Bi**	**apv-Bi**
-0.2	0.00	0.65	7.53	0.00	0.43	5.02
-0.3	1.41	7.28	12.80	0.94	4.85	8.53
-0.4	1.12	5.12	8.67	0.75	3.41	5.78